Research Article

A multiple-target mRNA-LNP vaccine induces protective immunity against experimental multi-serotype DENV in mice

Lihong He [a,c], Wenqiang Sun [a,b], Limin Yang [a], Wenjun Liu [a,b,c,d,*], Jing Li [a,c,*]

[a] CAS Key Laboratory of Pathogenic Microbiology and Immunology, Institute of Microbiology, Chinese Academy of Sciences, Beijing, 100101, China
[b] Institute of Infectious Diseases, Shenzhen Bay Laboratory, Shenzhen, Guangdong, 518000, China
[c] University of Chinese Academy of Sciences, Beijing, 100049, China
[d] Institute of Microbiology, Center for Biosafety Mega-Science, Chinese Academy of Sciences, Beijing, 100101, China

A B S T R A C T

Dengue virus (DENV) is a mosquito-borne virus with a rapid spread to humans, causing mild to potentially fatal illness in hundreds of millions of people each year. Due to the large number of serotypes of the virus, there remains an unmet need to develop protective vaccines for a broad spectrum of the virus. Here, we constructed a modified mRNA vaccine containing envelope domain III (E-DIII) and non-structural protein 1 (NS1) coated with lipid nanoparticles. This multi-target vaccine induced a robust antiviral immune response and increased neutralizing antibody titers that blocked all four types of DENV infection in vitro without significant antibody-dependent enhancement (ADE). In addition, there was more bias for Th1 than Th2 in the exact E-DIII and NS1-specific T cell responses after a single injection. Importantly, intramuscular immunization limited DENV transmission in vivo and eliminated vascular leakage. Our findings highlight that chimeric allogeneic structural and non-structural proteins can be effective targets for DENV vaccine and that they can prevent the further development of congenital DENV syndrome.

1. Introduction

Dengue, a mosquito-borne disease caused by dengue virus (DENV), which has four antigenically distinct serotypes (DENV-1, -2, -3 and -4) in the genus *Flavivirus* of the *Flaviviridae* family, is a growing threat to public health (Khetarpal and Khanna, 2016). Furthermore, multi-serotype co-infection may complicate prevention, diagnosis and treatment, especially in tropical and subtropical regions where DENV is endemic (Dhanoa et al., 2016). DENV infection induces lifelong protective immunity against primary infection serotypes of DENV, while modulating and mediating heterotypic secondary DENV infection and increasing the risk of developing severe dengue hemorrhagic fever and shock syndrome (Cui et al., 2021). Therefore, the quality of the antibodies induced by DENV vaccine candidates is more important, and it is urgent to explore a safe and effective DENV vaccine.

DENV is comprised of a spherical 50-nm virion containing three structural proteins [capsid (C), pre-membrane/membrane (prM/M), and envelope (E)], and a 10.7-kb capped RNA genome. E-DIII contains multiple type- and subtype-specific epitopes, eliciting only virus-neutralizing antibodies, and has been hypothesized to interact primarily with host cell receptors (Pokidysheva et al., 2006). In recent years, a growing study has accumulated that E-DIII is the key region of vaccine development perspective. Plasmids encoding E-DIII and recombinant E-DIII-based fusion proteins have been shown to induce neutralizing antibodies in laboratory animals (Chiang et al., 2012; Guzman et al., 2010). Similarly, the ability of recombinant E-DIII to diagnose dengue infection and induce neutralizing antibodies has been previously reported (Reddy et al., 2012). Together, these findings justify the selection of domain III for vaccine development. Non-structural protein 1 (NS1) in DENV 1–4 triggers endothelial barrier dysfunction, resulting in increased permeability of human endothelial monolayers in vitro (Modhiran et al., 2015). However, the pathogenicity of physiologically relevant amounts of NS1–C in vivo and vitro is blocked by NS1-immunized mouse polyclonal serum or NS1 monoclonal antibody and protected against lethal challenge by DENV, and anti-DENV-2 NS1 antibodies act on DENV-1 and DENV-4 infected cells (Beatty et al., 2015; Jearanaiwitayakul et al., 2020). Based on the fact that the NS1 of DENV serotype is highly conserved and not incorporated into mature dengue virions, we hypothesized that NS1 should not mediate antibody-dependent enhancement (ADE).

Clinical studies have shown that the balance between tetravalent immunity and all four antigens is the biggest challenge in DENV vaccine development (Guy et al., 2009). The neutralizing antibody (nAb) profiles of DENV1–4 and post-vaccination nAb attenuation are different in several candidate vaccine (Capeding et al., 2011). After a single dose immunization of TV003, DENV-1 had the lowest specific serum conversion rate and protective effect against type 2 serum (Kirkpatrick et al., 2016). Live attenuated CYD-TDV vaccine, which express the structural genes-encoding the PrM and E, showed less protective activity against serotypes 1 and 4 than DENV-2 and DENV-3 in phase I clinical trial (Barban et al., 2018). And CYD-TDV was proved to cause severe ADE and even immunogen imbalance in a previous phase IIb trial in Thailand (Sabchareon et al., 2012). In Takeda LAV vaccine (TAK-003), recent studies have shown that the nAb titers of the four serotypes are more asymmetric, with a stronger response to DENV-2 and a weaker response to DENV-4 (Sirivichayakul et al., 2016). Therefore, the ultimate goal of DENV vaccine design is to achieve as much immune homeostasis as possible under the premise of immune protection.

Recent advances have updated the mRNA vaccine development of many flaviviruses, such as Zika virus, tick-borne encephalitis virus, DENV, and Powassan virus (Wollner and Richner, 2021). Zika virus multi-target nucleotide modified mRNA vaccine can not only resist Zika virus and DENV infection but also prevent fetal microcephaly (Richner et al., 2017a, 2017b). These results are very encouraging for us to design DENV vaccine belonging to the same *Flavivirus* family. Importantly, the mRNA platform should be able to rapidly manufacture vaccine against multiple targets, as well as stimulate the innate immune system to achieve self-adjuvant action (Oberli et al., 2017). Studies of nucleoside-modified DENV mRNA vaccine coding for PrM/E or NS1 antigen demonstrate the potential of mRNA vaccine to prevent DENV infections by inducing protective immune responses and inducing durable T-assisted follicular cells and humoral immune responses in mice without positive effects (Zhang et al., 2020; Wollner et al., 2021; Roth et al., 2019). Impressively, the combination of E80 with NS1 not only enhanced the immune effect of the vaccine but also weakened the effect of ADE.

Our work is based on the hypothesis that mRNA vaccines both produce robust humoral immunity and trigger cellular immunity, which may enhance the effectiveness of DENV vaccine, while NS1 antibody can impair DENV infection in mice and might not mediate ADE. In this work, we designed mRNA vaccine that encodes a chimeric antigen E immunodominant region of DENV-1/4 (E-DIII, 303–395 aa) and an alloserotype DENV non-structural protein 1 (NS1, 1–302 aa) of DENV-2/3, with the combination of E1 + NS1-2 and E4 + NS1-3, then coating the mRNA with lipid nanoparticle (LNP). We evaluated the levels of DENV-specific neutralizing antibodies and T-cell immune responses induced by mRNA vaccine candidates and analyzed the challenge protection efficacy in immunocompromised C57BL/6 mice to obtain key parameters of vaccine safety and efficacy.

2. Methods and materials

2.1. Viruses, cells, bacterial strains and animals

The predominant serotypes of DENV, DENV-1 (Nauru/West Pac/1974, P17763), DENV-2 (Puerto Rico/PR159S1/1969, P12823), DENV-3 (Singapore/8120/1995, Q5UB51), and DENV-4 (Thailand/0348/1991, Q2YFH0) were propagated in C6/36 cells and stored at −80 °C at the Institute of Military Veterinary Medicine, Academy of Military Medical Science. The viral titers were determined based on baby hamster kidney (BHK-21, ATCC catalog no. CCL-10) cells, as previously described (Dai et al., 2021). The C6/36 cells were maintained in modified Eagle's medium (MEM, Gibco) supplemented with nonessential amino acids (Gibco) and 10% FBS at 28 °C with 5% CO₂. The BHK-21 cells and human embryonic kidney (HEK293T, ATCC catalog no. CRL-3216) cells were cultured at 37 °C in Dulbecco's modified Eagle's medium (DMEM, Life

Technologies) with 10% FBS (Gibco). *E. coli* strains (BL21) were cultured in Lysogeny broth (LB) medium (1% w/v Tryptone, 0.5% w/v yeast extract and 1% w/v NaCl) using a non-humidified shaker at 37 °C. Female mice of the C57BL/6 background were purchased from Beijing Vital River Laboratory Animal Technology Co., Ltd. (licensed by Charles River) and used between 6- to 8-weeks of age.

2.2. Generation of modified mRNA and LNP

The modified mRNA (methylpseudourine-5′-triphosphate instead of UTP) was synthesized from a linearized DNA template *in vitro* using a HiScribe™ T7 ARCA mRNA Kit (NEB). The mRNA was transcribed to contain the tissue-type plasminogen activator (tPA) signal peptide, transmembrane and cytoplasmic domain of vesicular stomatitis virus G (VSV-G) protein. Besides, the DNA template incorporates 5′ and 3′ untranslated regions (UTRs), and a poly-A tail were cloned into the pBluescript KS II (+) vector. In addition, a FLAG tag was added to the 3′ end of CDS to facilitate the later identification of target protein expression. Then the mRNA purified with an RNeasy Mini Kit (QIAGEN), and dissolved in RNase-free water. A Nano Drop microspectrophotometer (Thermo Fisher Scientific, USA) was used to determine the exact concentration of mRNA, and the purified mRNA was stored frozen at −80 °C until use.

LNP formulations were prepared according to a modified procedure, as previously described (Yanez Arteta et al., 2018). Briefly, lipids were dissolved in ethanol at molar ratios of 50:10:38.5:1.5 (ionizable lipid:DSPC:cholesterol:PEG-lipid). The lipid mixture was combined with a 50 mmol/L citrate buffer (pH 4.0) containing mRNA at a ratio of 3:1 (aqueous:ethanol), using a microfluidic mixer (Vancouver, BC) to obtain a lipid concentration of 12.5 mmol/L (1.85 mg/mL). Empty LNP was also prepared. Formulations were individually dialyzed in phosphate-buffered saline (pH 7.4) for >24 h. Then, the formulations were passed through a 0.22-μm filter and stored at 4 °C until use.

The LNP particle size and zeta potential were tested by DLS measurements using Malvern Instruments (Merck, Ireland), and the encapsulation and concentration of mRNA were determined using the RiboGreen assay (Thermo Fisher Scientific). The LNP were diluted and placed onto a copper grid, then washed twice with ddH₂O to remove excess salt ions. After 5 min, the grid was stained with 1% uranyl acetate, and transmission electron microscopy (TEM) was performed with a JEM-1400 instrument (JEDL, Japan) at an acceleration voltage of 80 kV. Digital micrographs were acquired using a 12M-B charge-coupled device camera (AMT BioSprint, Canada).

2.3. mRNA/LNP expressed and analyzed in vitro

mRNA was transfected to HEK293T cells with Lipofectamine 2000 Reagent (Life Technologies) based on the manufacturer's instructions (Shi et al., 2018). After a 24-h incubation, the cells were harvested and lysed for 30 min on ice. The whole cell supernatant was collected and analyzed by SDS-PAGE. Lysate samples were run on 12% Tris-HCl SDS-PAGE gels with subsequent transfer to PVDF (polyvinylidene fluoride) membranes, which were blocked in TBST (Tris-buffered saline, Tween 20) with 5% skim milk and 1% bovine serum albumin (BSA). PVDF membranes were incubated with a primary antibody (Anti-FLAG mouse mAb, Sigma; anti-His mouse mAb, Beyotime). The secondary antibody (horseradish peroxidase-conjugated goat anti-mouse IgG, Abcam) was added in blocking buffer for 45 min at 25 °C. After washing, PVDF membranes were incubated with hypersensitive luminescent solution (Solarbio), then imaged with an ECL system (CLINX, China).

LNP were directly added in cells and incubated for 24 h, then fixed in 4% paraformaldehyde 25 °C for 30 min. Then, the samples were blocked with 4% BSA (Fisher BioReagents) and stained with the anti-FLAG mAb (1:1000), 4E11 mouse mAb (1:1000) and 1A3 Rabbit (1: 1000). The secondary antibody (1:200) was Fluorescein isothiocyanate-conjugated goat anti-mouse IgG, or Tetramethylrhodamine-conjugated goat anti-

rabbit IgG followed by DAPI (4′,6-diamidino-2-phenylindole) staining for 15 min. The samples were observed using a Leica SP8 confocal laser scanning fluorescence microscope (Olympus, USA).

2.4. Protein expression and purification

The chimeric protein for specific antibody evaluation was expressed by prokaryotic (*E. coli,* BL21) expression system. The coding sequence (codon optimized for *E. coli*) for the E-DIII + NS1 were synthesized by Genscript (Nanjing, China). For gene cloning, the sequence was incorporated into the pET-22b (+) vector. In addition, $6 \times$ His tag was further added to the protein C terminus to facilitate protein purification. The sequencing-verified plasmid was subsequently transformed into *E. coli* BL21 cells to express the recombinant protein. For protein expression, the plasmid was firstly transformed into *E. coli* BL21, following induction with isopropylthio-β-galactoside (IPTG), the cultures were incubated at 16 °C for 24 h. Cells were lysed by sonication, and purification using Ni^{2+}-NTA-column was carried out according to protocol. Finally, the protein was exchanged into phosphate buffer (PH 7.2). The protein purity was detected by SDS-PAGE, Coomasie blue staining and rabbit anti-His antibody (Beyotime) Western blotting. In addition, E protein and NS1 protein used in our study was described in previous study (Liu et al., 2020).

2.5. Enzyme-linked immunosorbent assay (ELISA)

Corning Star flat-bottom 96-well plates were coated with 1 μg/mL E-DIII + NS1 or the separate E-DIII and NS1 protein in bicarbonate buffer (pH 9.6) at 4 °C overnight. Then, the plates were washed and blocked with 2% BSA for 1 h. Serum samples were serially diluted in blocking buffer and incubated for 2 h followed by five washes. HRP-conjugated IgG (total IgG, IgG1, IgG2a, Invitrogen) was diluted 1:5000 in blocking buffer and incubated for 1 h. Absorbance was measured at 450 nm using an ELISA reader (Thermo Fisher Scientific, USA). The OD value of the highest dilution was 2.1-fold higher than that of the negative control with the same dilution and was used as the serum endpoint dilution titer. Each subtype of ELISA includes a negative control serum and a serum to be tested. The serum to be tested was diluted according to the dilution gradient of total IgG to generate a complete titration curve of the test serum and control.

2.6. Focus reduction neutralization tests (FRNT)

Serial dilutions of heat-inactivated serum from vaccinated mice were incubated with 100 plaque forming units (PFU) of DENVs before infection of a monolayer of BHK-21 cells in 48-well plates. One hour after infection, cells were overlaid with 1% (wt/vol) methylcellulose in 2% fetal bovine serum (FBS) and minimal essential medium (MEM). Plates were fixed with 4% paraformaldehyde (PFA) after infection. Staining involved primary antibody 1A3 (500 ng/mL) and secondary antibody goat anti-mouse-HRP (200 ng/mL) in PermWash buffer (0.1% saponin and 0.1% BSA in PBS). Treatment with TrueBlue peroxidase substrate (KPL) produced focus-forming units that were quantified on an ImmunoSpot ELISpot plate scanner (Cellular Technology Limited, Canada). $FRNT_{50}$ are reported as the highest reciprocal dilution giving a focus count the 50% neutralization cutoff, and the geometric mean was computed for technical duplicates.

2.7. IFN-γ enzyme-linked immunosorbent spot (ELISPOT) assay and intracellular cytokine staining (ICS)

Spleen lymphocytes were seeded into anti-mouse IFN-γ mAb pre-coated 96-well plates at 2×10^5 cells (100 μL/well) and stimulated with 10 μg/mL purified protein for overnight incubation; phorbol 12-myristate 13-acetate (PMA) was used as a positive control. The ELISPOT assay was performed using a mouse IFN-γ ELISPOT Kit (Dakewe)

according to the manufacturer's instructions (Ranieri et al., 2014). Spots were counted using an immunospot reader (Cellular Technology Limited, USA).

Spleen lymphocytes (2×10^6 cells) were firstly stimulated for 2 h with 10 μg/mL of purified E1-DIII + NS1-2 and E4-DIII + NS1-3 protein as a specific antigen. Then the treated cells were continue cultured in the presence of 10 mg/mL monensin and brefeldin A in complete RPMI 1640 (Gibco) overnight. Stimulated cells were first incubated and stained with Fixable Dye eFluor 506 and the CD8-Percp-eFluor 710, CD3e-eFluor 450 (eBioscience), CD45-APC-Cy7, and CD4-FITC (BD Biosciences) surface markers. Then, cells were fixed in permeabilization buffer (Thermo Fisher Scientific) and stained with IFN-γ-PE-eFlour 610, IL-4-PE-Cyanine7, and TNF-α-APC (eBiosciences). All labeled lymphocytes were analyzed on a FACSAria III flow cytometer (BD Biosciences), and the data were analyzed using FlowJo V10.

2.8. DENV challenge in mice and measurement of viral load in blood

Immunizations with the LNP mRNA vaccine were administered via intramuscular injection in a 50 μL volume. Seven weeks after the initial vaccination, mice were challenged intravenously with 4×10^5 PFU DENV in 100 μL (ratio of DENV1–4 was 1:1:1:1). Anti-IFNαR1 blocking antibody (1 mg) to mice was administered one day prior to infection via intraperitoneal injection. Animals were monitored for weight loss. Blood was collected 2, 3 and 4 days post-challenge to determine viral loads in plasma. At day 4 after infection, mice were euthanized and harvested lung for tissue-related Evans blue dye analysis. Viral RNA in blood from challenged mice was detected by quantitative reverse transcription PCR (RT-qPCR). Briefly, Viral RNA in blood was extracted using the TaKaRa MiniBEST Viral RNA/DNA Extraction Kit (Takara) according to the manufacturer's protocol. DENV RNA quantification was performed by RT-qPCR targeting the *E* and *C* gene of DENV using SYBR Green Premix (Takara). The amplification was performed with an Applied Biosystems 7500 Real-Time PCR System (Thermo Fisher Scientific, MA, US). The primers used in our study were listed in Supplementary Table S3.

2.9. Quantification of Evans blue vascular leakage

Vascular leakage was quantified by Evans blue dye as previously described (Beatty et al., 2015). After a 4-day treatment, the mice were injected intravenously with 1% Evans blue dye (100 μL) and were sacrificed by cardiac puncture. Tissues were collected in pre-weighed tubes containing 1 mL of formamide and incubated at 37 °C and 5% CO_2. Evans blue concentration in extracts was quantified by measuring OD_{610} in samples and comparing to a standard curve. Data were expressed as nanograms of Evans blue dye per milligram of tissue weight.

2.10. ADE viral replication assay in vitro

Serum samples of immunized mice were heat inactivated and incubated with DENV (MOI = 0.1). After a 1-h pre-incubation, the resultant immune complexes (ICs) were mixed with K562 cells (ATCC catalog no. CCL-243, 5×10^4 cells/well) and incubated in a humidified 10% CO_2 incubator. The cells were washed once with DMEM, suspended in fresh 2% FBS (200 μL/well), and returned to the incubator. After a 48-h incubation to allow viral replication and egress, the cells were centrifuged, and the infection percent was determined via flow cytometry (BD Biosciences).

2.11. Statistical analysis

All data were presented as the mean ± standard error of the mean. Statistical significance was determined using one-way ANOVA multiple comparisons. All graphs were generated with GraphPad Prism version 6.0 software.

3. Results

3.1. Characterization of DENV mRNA vaccine candidates

We developed a multi-target vaccine platform to generate optimized LNP for intramuscular delivery of the modified mRNA envelope. The final cellular location of the antigen is determined by the signal peptide and transmembrane domain (Maruggi et al., 2019). This may be inherent in the natural protein sequence, or it may be designed to guide the protein to the desired cellular compartment. Moreover, high expression and secretion of target protein *in vivo* may ensure good immunogenicity. The tissue-type plasminogen activator (tPA) has been used as an exogenous lead sequence to drive target proteins into the cellular secretory pathway, while VSV-G protein effectively mediates membrane fusion and anchor-choring in the transmembrane (TM) domain and cytoplasmic domain (Costa et al., 2006; Golden et al., 2008; Okimoto et al., 2001).

E-DIII of DENV-1 and DENV-4 with low seroconversion rate were selected as immunogens to achieve a satisfactory balance between virulence and immunogenicity (Barban et al., 2018). Anti-DENV2 $NS1_{1-279}$ antibody showed higher antiviral activity against DENV-1 than DENV-4 (Jearanaiwitayakul et al., 2020). Thus, E-DIII (DENV-1) + NS1 (DENV-2) and E-DIII (DENV-4) + NS1 (DENV-3) were selected as the immunogenic combination. To efficiently express the target protein on the surface of the cell membrane, we designed a modified mRNA encoding a type 1 (N7mGpppAm) cap, the tPA signal and VSV-G TM and CD, 5′ and 3′ untranslated sequences and optimized target antigen E-DIII and NS1 (Fig. 1A). To select representative conserved broad-spectrum DENV antigens, E-DIII (303–395 aa) and NS1 (1–302 aa) sequences from the past 10 years were downloaded and compared (Supplementary Table S1).

Subsequently, the 3D structure and linear epitope of B cells were predicted using the AlphaFold Protein Structure Database (AlphaFold DB, alphafold.ebi.ac.uk) and the Immune Epitope Database (IEDB, iedb.org) (Supplementary Fig. S1; Supplementary Table S2). Five highly conserved motifs were found in the chimeric proteins. These results indicated that highly conserved epitopes were located on structure surfaces (Supplementary Fig. S2). Under the guidance of signal peptides and membrane extension domains, we conducted a reduced graphs of expression processing of membrane expressed proteins *in vivo* (Fig. 1B). Co-incubation of 293T cells by mRNA transfection or LNP resulted in efficient expression and protein membrane localization, as judged by IFA (Fig. 1C, Supplementary Fig. S3), Western blotting (Fig. 1D). The mean size of the LNP was less than 100 nm in diameter, additional analysis performed using transmission electron microscopy (TEM) supported the DLS data, showing small and uniform size distribution of the particles (Fig. 1E).

3.2. Screening of optimal immune dose of DENV mRNA vaccine candidates in mice

To select the optimal vaccine dose, the mice aged from 6 to 8 weeks were immunized with DENV-a mRNA, DENV-b mRNA, or empty LNP and boosted with the same LNP at 2 week intervals (Fig. 2A). Mice receiving 5 or 20 µg doses of the DENV-a and DENV-b LNP showed similar endpoint titers at 8 weeks after initial vaccination. The antibody titer of the 2 µg dose induced the lowest antibody titers in both of the immunized group (Fig. 2B and C, Supplementary Fig. S4B). DENV-a elicited DENV-1 E-DIII specific IgG, with the average endpoint titer of 512, 7864 and 15,264 in the 2 µg, 5 µg and 20 µg group (Fig. 2B). The immunization group produced antibody titers against NS1 protein with 2360, 38,400 and 61,440, which was basically the same as that of the chimeric protein (Supplementary Fig. S4B). Likewise, the DENV-b immunized group also produced highly specific antibodies for DENV-4 E-DIII protein and DENV-3 NS1, the mean endpoint titer with E-DIII showed 768, 4096 and 4608, then the titer was 2560, 19,472 and 32, 768 when coated NS1 of DENV-3 (Fig. 2C). This means that total antibodies targeting NS1 are slightly higher than that of E-DIII, but not significantly different.
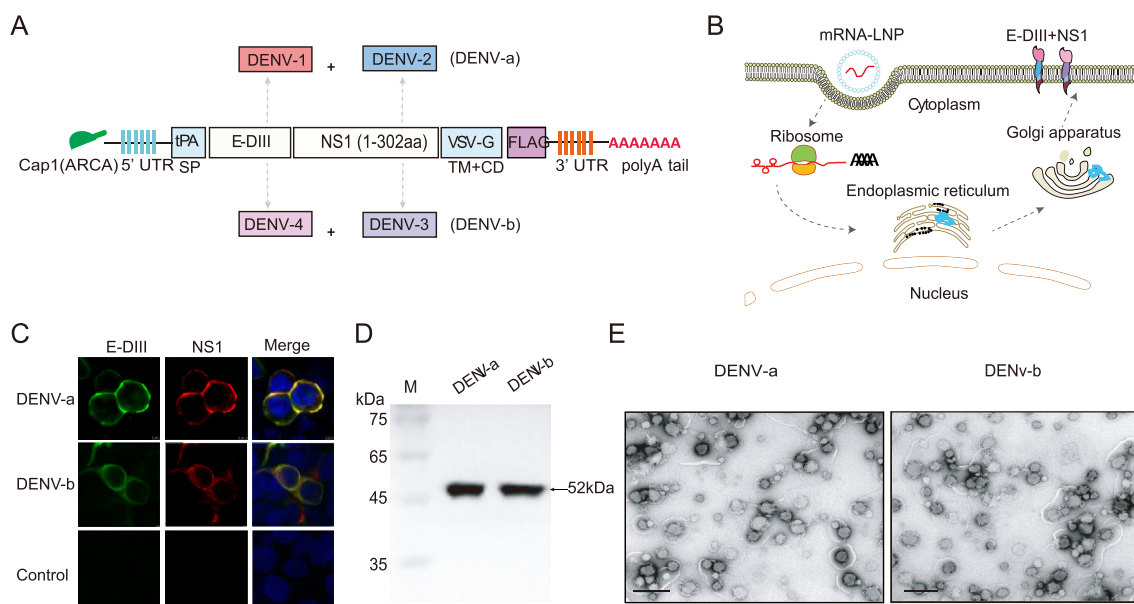

Fig. 1. Design and evaluation of physicochemical properties of dengue virus (DENV) mRNA vaccine candidates. **A** Schematic diagram of the construction of two DENV mRNA vaccine candidates. Through codon optimization, the heterochimeric E-DIII and NS1 constructs were fused to an N-terminal tPA signal sequence (tPA), a C-terminal vesicular stomatitis virus G protein transmembrane and cytoplasmic domain (VSV-G TM + CD), and cloned into a DNA plasmid. The combination of serotype 1 (DENV-1) and serotype 2 (DENV-2) is named DENV-a, and DENV-b is formed by the chimera of serotype 3 (DENV-3) and serotype 4 (DENV-4). **B** Schematic diagram showing the proposed mechanism for mRNA vaccine candidate translation in cytoplasm. The dotted arrows indicate the order in which the proteins are translated for processing. **C** Immunofluorescence co-localization of DENV-a and DENV-b expressing viral proteins. The E-DIII (Green) was labeled using the mAb 4E11, the NS1 (Red) was detected with 1A3. The nuclei were stained with DAPI (blue). Scale bar, 25 µm. **D** Western blotting was used to detect HEK-293T cells transfected with DENV-a and DENV-b lipid nanoparticle-encapsulated, nucleoside-modified mRNA (mRNA-LNP) for 24 h. The first column represents the molecular mass (M) of the protein. **E** Transmission electron microscopy images showing representative DENV-a and DENV-b nanoparticles, respectively (scale bar, 100 nm).
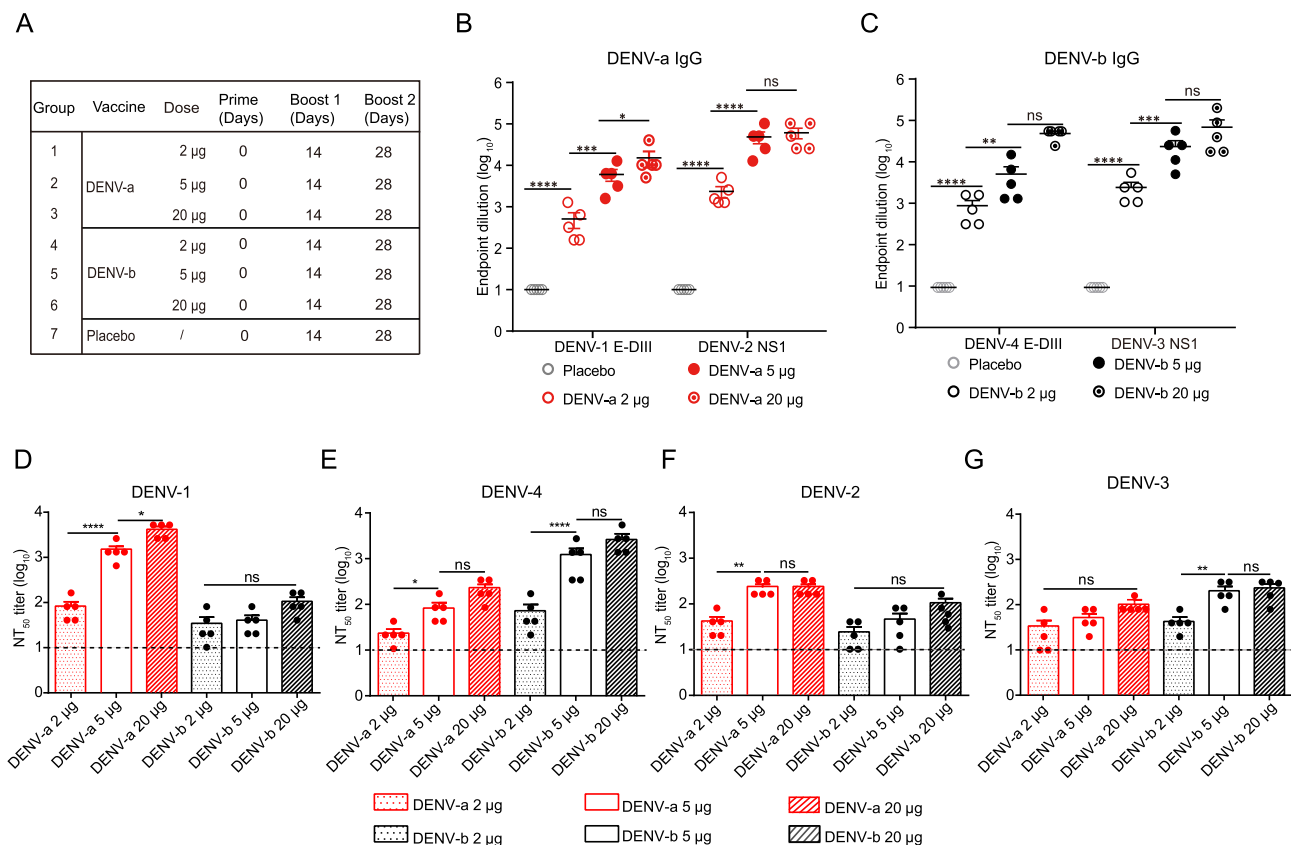
Fig. 2. Screening of different doses of DENV mRNA candidate vaccine. **A** Grouping of vaccine candidates at different doses (2, 5, and 20 μg). Female C57BL/6 mice (n = 5) aged from 6 to 8 weeks were immunized every 2 weeks, and serum was collected for analysis at 6 weeks after enhanced immunization. Endpoint dilution titers of each group were measured by ELISA plates coated with DENV-1 E-DIII and DENV-2 NS1 protein (**B**), DENV-4 E-DIII and DENV-3 NS1 protein (**C**). The empty-LNP group was given a placebo. **D–F** Neutralizing antibody titers against DENV-1(**D**), DENV-2 (**E**), DENV-3 (**F**), and DENV-4 (**G**) were analyzed using the FRNT$_{50}$ assay. The dashed line indicates the detection limit. Data are presented as means ± SEM. Significant differences were determined by one-way ANOVA (*$P < 0.05$, **$P < 0.01$, ***$P < 0.001$ and ****$P < 0.0001$; ns indicates not significant).

As shown in Fig. 2D, the sera of mice inoculated with the DENV-a vaccine candidate produced a moderate neutralizing antibody response to DENV-1 at doses ranging from 2 to 20 μg, with an average 50% FRNT$_{50}$ of 1:80, 1:2560 and 1:5120. As expected, DENV-b immune sera were highly neutralizing titers with DENV-4, with a 32-fold difference between the 2 μg- and 5 μg-dose groups. Specifically, these FRNT$_{50}$ values were comparable with DENV-a in DENV-1 serum. The DENV-b group displayed neutralization titer with DENV-4 were 1:68, 1:1152 and 1:2560, respectively (Fig. 2E). It should be noted that although the chimeric non-structural proteins had neutralizing activity against DENV-2 and DENV-3, the mean titer (1/324 and 1/308) of 5 μg-dose group, which showed no significant difference among each dose group (Fig. 2E and F), but 10- to 100-fold lower than DENV-1. We also analyzed the difference of neutralization titer between different serotypes. There was no difference in neutralization titer between DENV-1 and DENV-4, and no difference in neutralization titer between DENV-2 and DENV-3. DENV-2 was significantly different from DENV-1 and 4, while the same goes for DENV-3. Therefore, the chimeric vaccines of structural and non-structural proteins in heteromorphic serum yielded good immunogenicity, and vaccine candidate dose screening tests showed that the 5 μg-dose group was sufficient to produce considerable cross-neutralization.

3.3. The mRNA vaccine candidate elicited humoral immune responses and cytokine profiles of T lymphocytes

To test the persistence of antibody, intramuscular injection of a 5-μg dose was used to immunize mice. In the humoral reaction, serum was collected at a specified time to detect the level of anti-protein-specific IgG

antibody. As expected, mice mmunization with DENV-a, DENV-b and DENV-ab mRNA-LNP induced neutralizing antibodies with NT$_{50}$ approached ~1/96 and ~1/3328 at day 42 post immunization. Remarkably, DENV-ab serum neutralization titres are relatively high in all four serotypes (Fig. 3A–D). The antibody levels in DENV-ab mice were highest at 6 weeks, significantly higher than those in the DENV-a and DENV-b groups, with titers peaking at 6 weeks after the increase in all immunized groups and continuing to maintain at 30 weeks after the initial inoculation (Supplementary Fig. S5). The long-lasting humoral immune response of each mRNA vaccine to E-DIII (DENV-1, DENV-4) and NS1 (DENV-2, DENV-3) full-length proteins were also assessed. Similarly, endpoint titers in all groups were higher for NS1 than for E-DIII protein (Fig. 3E–G, Supplementary Fig. S6). In DENV-ab mRNA group, the endpoint titer reach maximum at week 6, both DENV-2 NS1 and DENV-3 NS1 have higher antibody titers than E-DIII protein (Fig. 3G). As expected, mice mmunization with DENV-a, DENV-b and DENV-ab mRNA-LNP induced neutralizing antibodies with NT$_{50}$ approached ~1/96 and ~1/3328 at 42 days post immunization. Remarkably, DENV-ab serum neutralization titres are relatively high in all 4 serotypes (Fig. 3E–G). To determine the dominant immune response, E-DIII and NS1 IgG subtypes were measured, since the proportion of different subtypes was determined by the dominant cytokine environment. As shown, increased IgG2a in response to Th1 cytokine IFN-γ was significantly higher than increased IgG1 in response to Th2 cytokine IL-4 (Fig. 3H–J). In all assay groups, there was a significant difference in specific IgG 2a/IgG 1 except the DENV-4 E-DIII group. Thus, mRNA vaccine-induced Th1 dominant vaccine response was confirmed. The results of serum assays demonstrated that mice immunized with the DENV-ab vaccine had a good
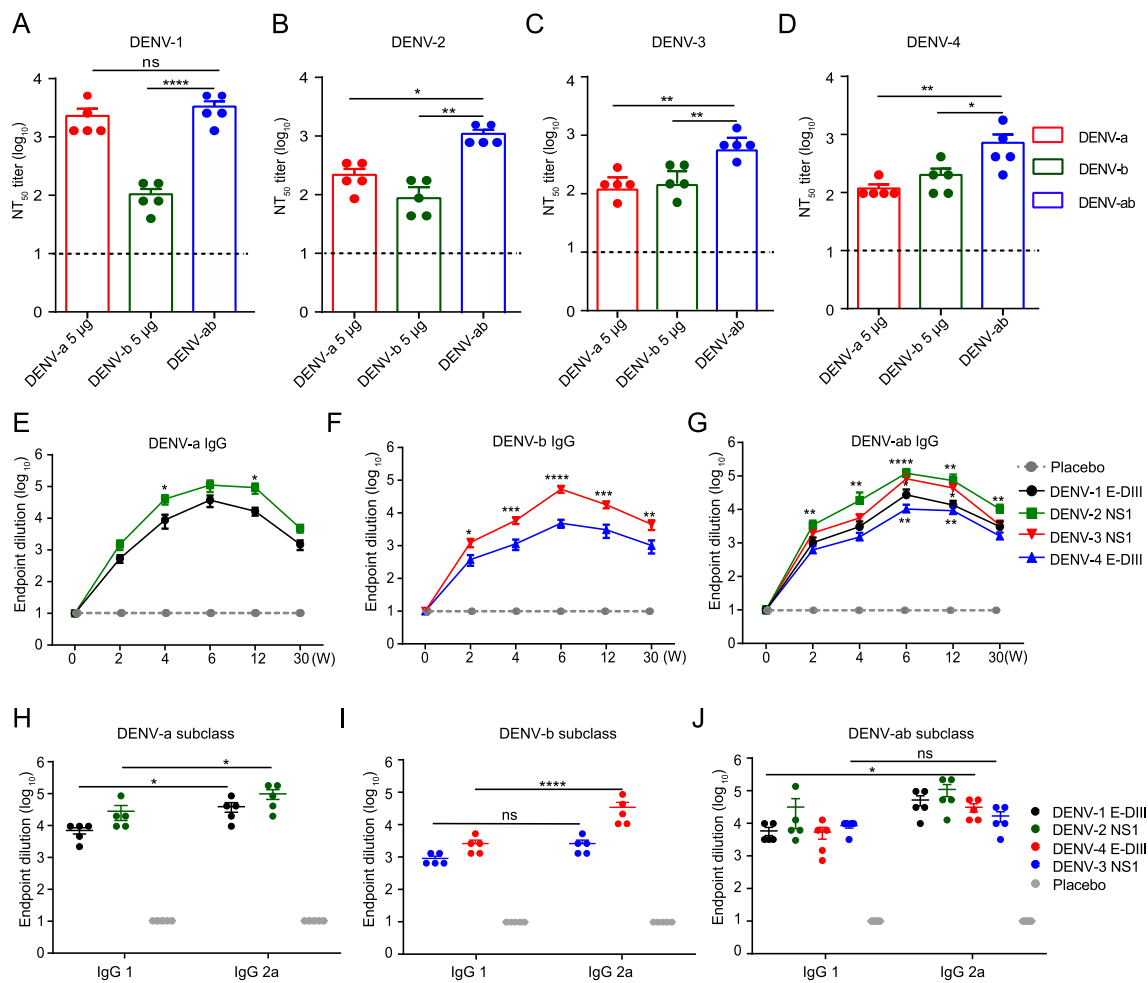
Fig. 3. Continuous humoral immune evaluation of DENV vaccines candidates. DENV-a, DENV-b, and DENV-ab vaccines candidates (5 μg) were intramuscularly injected into female mice aged from 6 to 8 weeks (n = 5). Serum was collected at the specified time to determine the antibody neutralization titers and endpoint titers. (A–D) Neutralization titers of serum of immunized mice against DENV-1 (A), DENV-2 (B), DENV-3 (C), and DENV-4 (D) were analyzed by $PRNT_{50}$ assays at 6 weeks after prime vaccination. (E–G) End-point titers of E-DIII and NS1 specific IgG subclasses in mice of DENV-a (H), DENV-b (I) and DENV-ab (J) after booster immunization with 5 μg mRNA vaccine (week 6). W on the X-axis on represents weeks. (H–J) The Th1/Th2 dominance determined as the end-point titers of IgG2a and IgG1. All of the significant differences were relative to the DENV-ab group. Data are presented as means ± SEM. Significant differences are shown as $*P < 0.05$, $**P < 0.01$, and $****P < 0.0001$; ns indicates not significant.

neutralization titer among the four serotypes. These data proved that a 5 μg can be a good immunization dose in our study.

To study the cellular immune response to the specific antigen, immune cells were obtained from the spleen cells of vaccinated mice at 30 weeks after the initial immunization. The ELISPOT results showed that both vaccine candidates activated T lymphocytes and secreted IFN-γ; the spots in the DENV-ab group were higher than in the other vaccine groups, especially compared to the placebo group (Fig. 4A, Supplementary Fig. S7D). To further investigate cell-mediated immunity, the levels of cytokines (TNF-α, IFN-γ, and IL-4) secreted in the supernatant of cultured splenocytes were quantified by flow cytometry. The IFN-γ percentage of $CD4^+$ T cells in the DENV-a group was significantly higher in the empty LNP group, and the IFN-γ percentage of $CD8^+$ T cells was slightly higher than in the placebo group (Fig. 4B and C, Supplementary Fig. S7C). In addition, cytokines play a key role in the development of innate responses by enhancing the adaptive immune response, such as IFN-γ, IL-4, and TNF-α (Fig. 4D). Our data demonstrated that the Th1 response was activated with the specific IgG2a and IgG1 ELISA. In general, both vaccine stimulated cellular immune responses, primarily the Th1-biased response. In summary, both mRNA vaccine candidates induced cellular immune responses, and DENV-ab was the best candidate vaccine for broad spectrum protection.

3.4. The DENV-ab mRNA vaccine candidate afforded protection against DENV challenge in mice

Co-infection with multiple DENV serotypes has been reported where multiple dengue serotypes co-circulate (Mishra et al., 2017). Furthermore, the high percentage of co-infection with multiple serotypes were also observed with increased disease severity (Biswal et al., 2019). Shockingly, a triple infection with DENV-2, -3 and -4 in the human blood sample was found recently (Rai et al., 2021). Validation of mouse models of DENV infection depends on validation of viremia and replication in infected mouse tissues (Plummer and Shresta, 2014). In addition, the level of DENV viremia is one of the most important factors determining the infectivity of the virus to humans via mosquitoes (Matangkasombut et al., 2020). The recombinant DENV transmission cycles in mice and mosquitoes studies by Christofferson et al. showed that on day 3 post-infection, infected mice have the highest titers of viremia and could feed on mosquitoes and transmit the virus (Christofferson Rc et al., 2013). Immunocompetent 6–8 week-old female C57BL/6 mice were immunized with DENV-ab LNP and boosted with the same LNP two weeks later (Fig. 5A). At six weeks after initial vaccination, serum was analyzed for ELISA and neutralizing activity using DENV. Mice receiving DENV-ab showed neutralization titers with 1:2560, 1:1792 of DENV-1
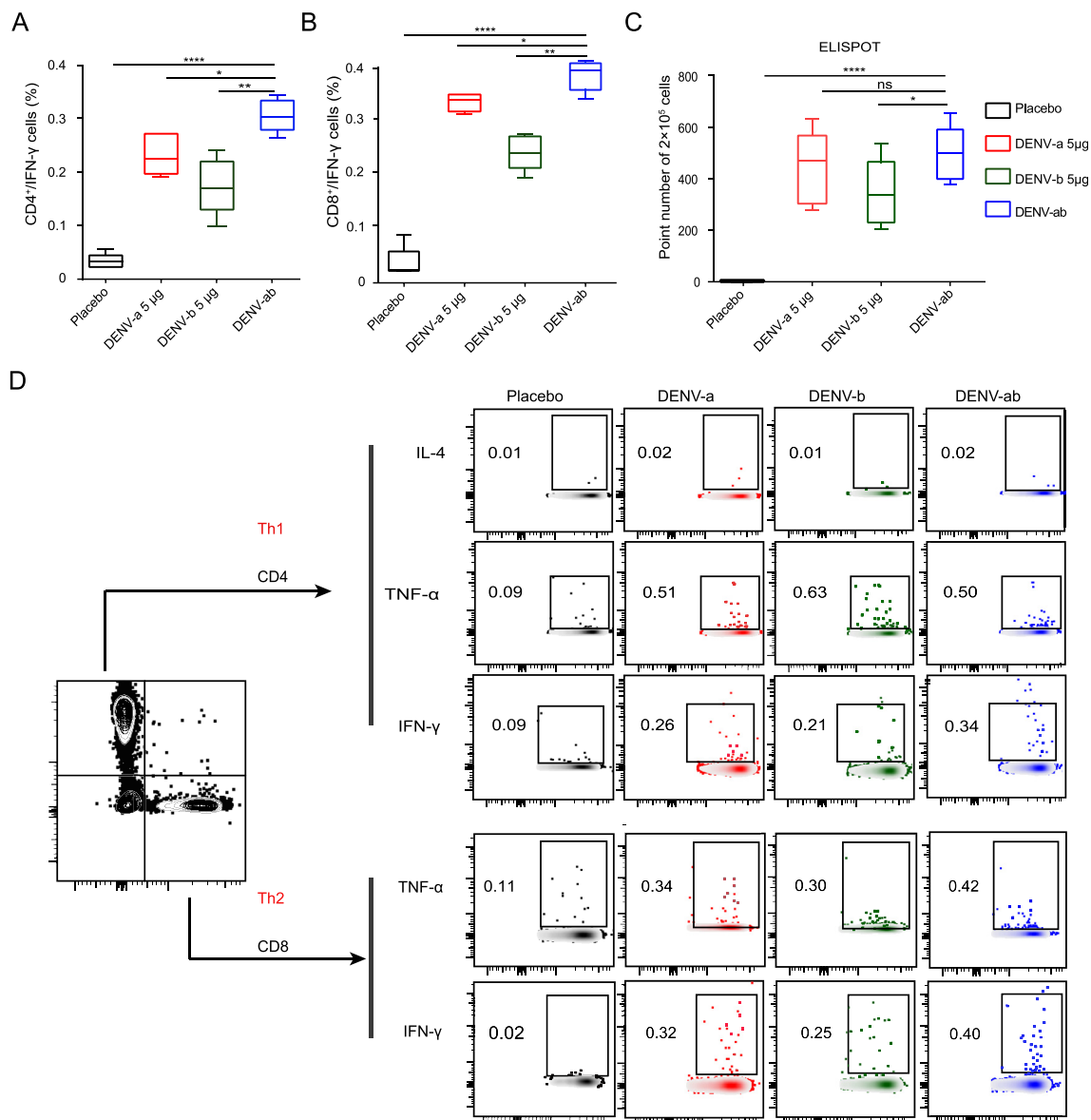
Fig. 4. Cytokine profile of responses induced by vaccine candidates. Spleen cells were re-stimulated with chimeric E-DIII + NS1 protein, and cytokine secretion was analyzed by fluorescence-activated cell sorting and ELISPOT assays at 30 weeks after enhanced immunization (n = 5). All tests were independent and included positive and negative controls. (**A, B**) FCM analysis of the intracellular cytokine IFN-γ induced by CD4$^+$T cells and CD8$^+$T cells after stimulation with mRNA-LNP vaccine candidates. **C** The IFN-γ secretion of 2×10^5 spleen cells was determined by ELISPOT assays upon re-stimulation with 10 μg/mL of E-DIII + NS1 chimeric protein. **D** Representative FCM analysis plots of intracellular cytokines and gates from single mice in each group. Each mouse had a total of 2×10^6 cells. Cells were pre-gated on live/dead-CD45$^-$CD3$^-$CD4/CD8. Data are presented as means ± SEM. Statistical analysis was performed using one-way ANOVA. (*$P < 0.05$, **$P < 0.01$, and ****$P < 0.0001$; ns. indicates not significant).

and DENV-4, the titer of DENV-2 and DENV-3 was 1:320 and 1:304 (Fig. 5B). The total IgG titer varied ~10^3 to 10^5 (Fig. 5C). To establish a co-infection challenge model, we passively transferred 1 mg of the blocked anti-IFN-αR1 antibody to C57BL/6 mice one day before they were challenged intravenously with 4×10^5 PFU DENV (ratio of DENV 1–4 was 1:1:1:1) at ~7 weeks after initial vaccination. The mice inoculated with empty-LNP vaccine began to lose weight on day 3 after infection, while those inoculated with DENV-ab mRNA-LNP vaccine maintained stable and slightly increased weight after infection (Fig. 5D). At day 2 after infection, blood was collected and analyzed for viremia by qPCR. Mice vaccinated with the DENV-ab vaccine showed slightly measurable viremia on day 2 after infection with DENV, the mean peak virus titers with 0.4 ± 0.1, 0.3 ± 0.2, 0.4 ± 0.2 and 0.1 ± 0.1 of DENV-1, -2, -3 and -4, respectively (Fig. 5E). Whereas the placebo immunized

animals had viremia was detected on day 4 after infection (Fig. 5E). The mice were euthanized at day 4 after infection, and their lungs were harvested for tissue-related Evans blue dye analysis to quantify circulatory leakage during intravenous injection. Consistent with their high neutralizing titers, mice vaccinated with DENV-ab LNP showed breakthrough reduced levels of Evans blue staining in the lung, the levels were at least 10-fold lower than observed with placebo (Fig. 5F). As shown in Fig. 5G, the lung tissue of the PBS control group showed a clear blue leak after injection of Evans blue, though there was no significant difference between the lung tissues of the vaccine group and PBS injection group, these data demonstrate a role for NS1 alone in inducing vascular permeability *in vivo*. Therefore, DENV-ab LNP can not only inhibit vascular permeability in co-infected mice, but also block experimental ability of viremia induced by DENV infection in mice.
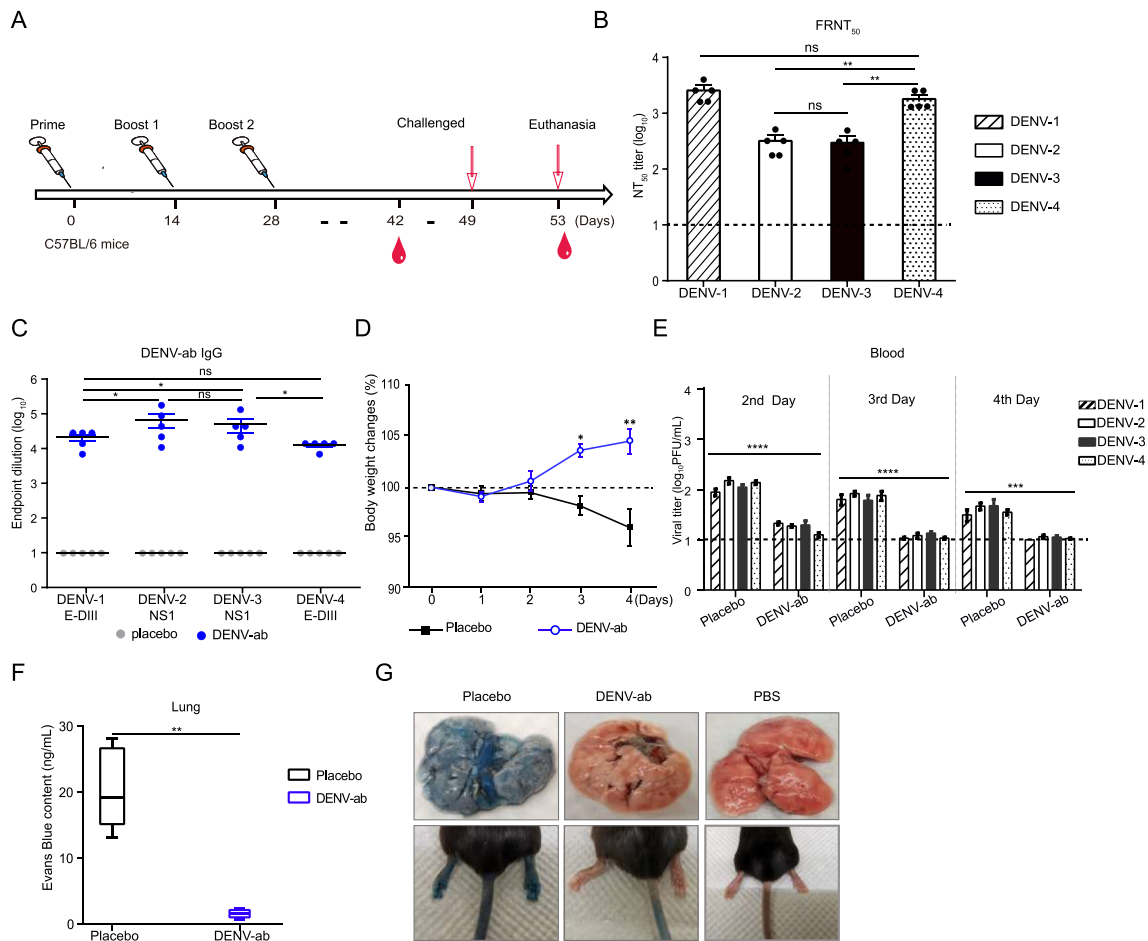
Fig. 5. Evaluation of challenge protection in vaccine-immunized mice. **A** Flow chart of the animal experiment. Three weeks after immunization enhancement, C57BL/6 mice (n = 5) were subcutaneously inoculated with a total of 4×10^5 PFU of DENVs (the PFU ratio of the four viruses was 1:1:1:1:1). One day before immunization, C57BL/6 mice were intraperitoneally inoculated with 1 mg of anti-IFNαR1 monoclonal antibody. Lungs were collected at 4 days post-infection (dpi). NT_{50} titers against DENV (**B**) and endpoint titers of IgG (**C**) were measured by $FRNT_{50}$ and ELISA assays. Body weight changes (**D**) and viral titers in blood (**E**) were recorded on 2, 3, and 4 dpi. **F** Quantification of Evans blue dye extracted from the lungs of DENV-infected mice treated with vaccine or empty LNP. Lung tissue was collected and soaked in 1 mL formamide to determine the absorbance value at OD_{610}. **G** Representative images of Evans blue-stained lung tissue from mice. PBS is shown as a negative control. Data are presented as means ± SEM. Statistical analysis was performed using one-way ANOVA (*$P < 0.05$, **$P < 0.01$, and ***$P < 0.001$; ****$P < 0.0001$; ns indicates not significant).

3.5. The DENV-ab mRNA vaccine candidate had good safety by ADE assays

To evaluate whether the NS1 component against the chimera of the E-DIII-based vaccine could both elicit specific antibody and attenuate the ADE response, the antibody and pre-immune DENV complex were incubated with Fcγ receptor-positive K562 cells. As shown in the representative results in Fig. 6, the peak percentage of DENV-1-infected cells peaked at 6.0% at a 1:10, 240 dilution of DENV-a serum samples incubated with DENV-1. By contrast, the level of infection (7.59%) was not significantly increased in the sera of mice immunized with DENV-ab mRNA at 1: 10,240 dilution (Fig. 6A). As the result shown, the mean titer of DENV-ab serum to DENV-4-infected cells reached 8.8% at 1:10, 240, and there was no significant difference between DENV-ab serum and other sera. The data indicated that the mixed immune response induced by E-DIII + NS1 mRNA vaccine candidate did not significantly enhance ADE activity in DENV infection. Surprisingly, serum from mice immunized with DENV-ab mRNA displayed no significant difference with the separate DENV-a or DENV-b immune sera in DENV-2 and DENV-3 group (Fig. 6C and D). Together, these data reinforced the notion that neutralization titers are negatively correlated with ADE capability. They also proved that the NS1 fusion vaccine has a neutralization effect and

can partially attenuate the ADE effect (Zhang et al., 2020), indicating is as an effective candidate vaccine for broad-spectrum DENV vaccine.

4. Discussion

DENV continues to have a major impact on public health systems worldwide, particularly in tropical and sub-tropical regions. The need for and development of a vaccine has been the number one priority for preventing the disease, but many bottlenecks remain. In early DENV vaccine studies, live attenuated vaccine was the main means to prevent infection (Bhamarapravati and Sutee, 2000). However, there are concerns about the risks of revirulent strains of traditional vaccine (Martinez et al., 2021).

Previously promising live attenuated tetravalent DENV vaccine, LATV and TAK-003, have been tested *in vivo* and even clinically, regardless of contact with flaviviruses (Guirakhoo et al., 2001). LATV is safe in children and adults, however the amount of DENV-2 needs to be increased to achieve balanced seroconversion (Kirkpatrick et al., 2015; Durbin et al., 2020). Similarly, TAK-003 induces seroconversion, in which the neutralizing antibody is active against all four DENV serotypes, while induces lower antibody levels to DENV-3 (Sáez-Llorens et al., 2018; Jackson et al., 2018). Serotype cross-reactive immune response and
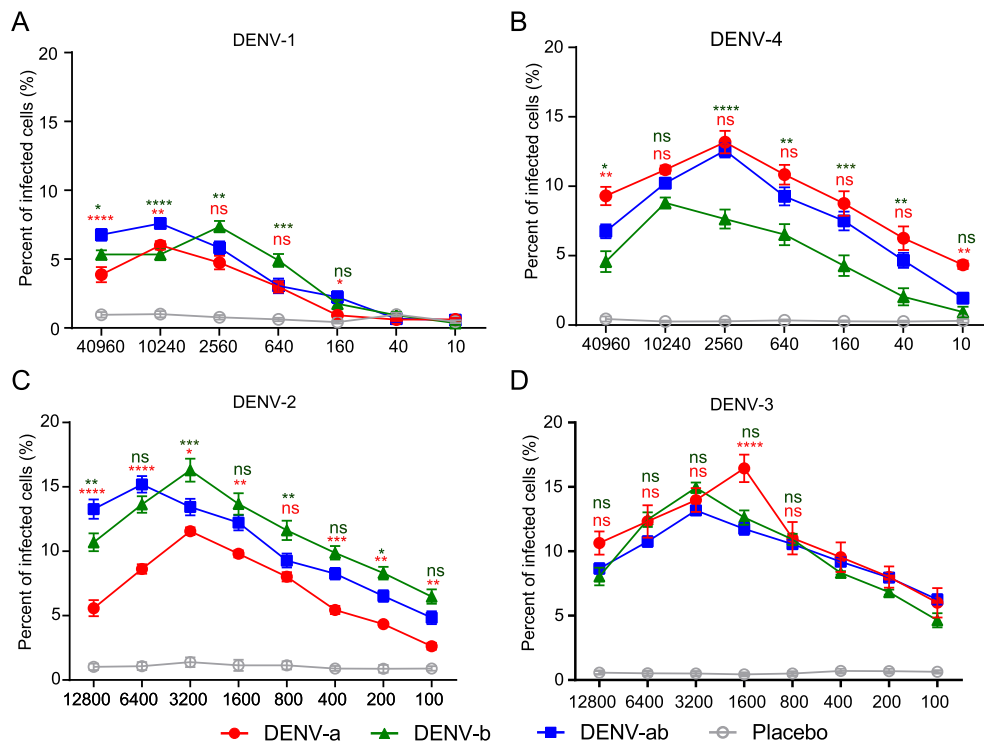
Fig. 6. Antibody-dependent analysis of DENV 1–4 infection in K562 cells with monotype vaccine candidate and mixed vaccine candidate, respectively. C57BL/6 mice were immunized with 5 μg monotype vaccine candidate (DENV-a and DENV-b) or mixed vaccine candidate (DENV-ab) mRNA LNP and mixed with DENV-1, DENV-2, DENV-3, and DENV-4 in serially diluted serum at week 6 and incubated with Fc-γ receptor expressing K562 cells. The cell infection was quantitated by flow cytometry (FCM). Representative curves for each serotype are shown for groups **A**, **B**, **C**, and **D**. All significant differences were relative to the DENV-ab group. Red represents comparisons between DENV-ab and DENV-a, and green represents differences with DENV-b. Data are presented as means ± SEM. Significant differences were determined by one-way ANOVA (*$P < 0.05$, **$P < 0.01$, and ***$P < 0.001$; ****$P < 0.0001$).

cellular response levels are key factors in DENV vaccine evaluation. In our study, serum from DENV-a, DENV-b, or DENV-ab vaccine candidates displayed considerable cross-neutralizing antibodies against all four DENV, and DENV-ab conferred a stronger cross-neutralizing titer than single vaccine. At a 10-μg dose, neutralizing antibody titers of the mRNA vaccine candidate encoding full-length DENV-1 or DENV-2 PrM/E or E80/NS1 produce NT_{50} titers of ~10^2 and ~10^2–10^4 in mice, respectively (Wollner et al., 2021; Zhang et al., 2020). Consistent with the neutralizing titer of these single serotype vaccine candidates, antiviral antibodies are sufficient for protection.

It is well known that one of the difficulties in DENV vaccine evaluation is broad spectrum activity. Although DENV-ab could limit transmission of DENV in mice and eliminate vascular leakage, the lower titer of neutralizing antibodies against DENV-2 and DENV-3 should not be ignored. In subunit vaccines, D-PIGS targeting E-DIII exhibits extensive and low neutralizing antibodies to DENV 1–4 (Kim et al., 2018). Our vaccine target on E-DIII also exhibited broad spectrum activity but a relatively low level of neutralizing antibodies compared to other vaccine. One of the limitations of the antigen design may be due to the incomplete immunogenicity of the E protein (Thomas et al., 2020; Zhang et al., 2020). Therefore, additional research is needed to investigate how to avoid ADE while ensuring complete immunity of the E protein.

The interesting finding is that single mRNA LNP at doses as low as 5 μg could elicit the same immune response as the 20 μg-dose, which may be affected by antigen stability, uptake restriction, or even translation efficiency in mice. A similar report was found in previous studies, i.e., that 5 μg DENV-2 mRNA LNP induced an immune response in mice similar to the 20 μg-dose (Zhang et al., 2020). As well, 2 μg ZIKV prM/E-mRNA induced neutralizing antibody titers with a $PRNT_{50}$ of approximately 10^5, comparable to a 10 μg-dose (Richner et al., 2017a).

The complex mechanism and related factors of antigen translation and presentation *in vivo* deserve further study.

In addition to focusing on antibodies produced by B cells, T-cell immunity appears to have a crucial protective role in both animals and humans, due to their characteristics (Grifoni et al., 2020). For the antibody responses to DENV infection mainly target the prM, E and the secreted glycosylated NS1 antigen. While, the cellular responses primarily target NS3, NS4 and NS5 (Roth et al., 2019). According to our results, the DENV-ab treatment simultaneously induced activation of both Th1 $CD4^+$ T cells and $CD8^+$ T cells. Bal et al. demonstrate that surface-displayed Co1-scEDIII-AGA preparations induce a strong immunogenicity compared to non-displayed scEDIII-Co1 (Bal et al., 2018). Our results indicated that fusion of the transmembrane region and cytoplasmic domain of vesicular stomatitis virus G protein to the C-terminal of the chimeric antigen ensures transmembrane protein transfer during construction. We hypothesized that vaccine formulations with the transmembrane region and cytoplasmic domains would result in moderate antigen expression and lower antiviral antibody titer but a greater T cell immune response compared to other DENV mRNA LNP.

Inevitably, for the development of DENV vaccine, immune imbalance caused by replicative vaccine is a key factor in ADE production in DENV-naive individuals (Elong Ngono and Shresta, 2019; Nivarthi et al., 2021). The main concern is that the E-DII-mutated E protein does not effectively reduce ADE effects in the mRNA vaccine platform but leads to incomplete immunogenicity (Wollner et al., 2021). It should be noted that ADE of DENV-2 and DENV-3 in the serum of our immunized mice was 5%–10% at 1:100, comparable to the level induced by a full-length deleted vaccine of DENV-1 (Wollner et al., 2021). DENV-a, DENV-a, and DENV-ab showed a peak of 15%–20% when infected with heterologous DENV, which was lower than the serum dilution titer (15%–60%) at the peak of

DENV-2 mRNA vaccine treatment conducted by Zhang et al., suggesting the importance of NS1 in the formulation of DENV vaccine (Zhang et al., 2020). However, the ADE effect of NS1 or E-DIII protein immune serum alone and the comparative analysis and evaluation of polyvalent vaccine should be considered and further research direction.

One of the challenges of DENV vaccine evaluation is the difficulty of developing animal models for preclinical studies that can be widely applied to human diseases (Milligan et al., 2017). Compared with C57BL/6, AG129 mice lacking interferon α/β and γ receptors have proved to be a valuable model of infection (Sarathy et al., 2015). However, AG129 mice lack certain aspects of cellular immunity that may affect their ability to produce protection after immunization with non-replicating vaccines (Zuest et al., 2015). Therefore, a combination of different models should be used to comprehensively evaluate the protective effect of the DENV vaccine, and the application of only one animal model is the limitation of our study. For viral titer testing, many studies have reported PCR as a rapid, sensitive and non-invasive method for the detection of flavivirus infection, especially in DENV detection (Gomes--Ruiz et al., 2006; Paudel et al., 2011). From the animal welfare protection perspective, viral load indicates that the protective effect of the vaccine can reduce animal suffering and, to a certain extent, waste of laboratory animals. Of course, there are some weakness in the way viral load indicates the efficiency of vaccine protection compared with gold standard for lethal protection. Viral load only reflects the efficiency of virus replication or clearance, not the degree of damage to the body. When only *in vivo* viral replication is needed to characterize, viral load is a relatively good measure compared to traditional standards.

In recent years, mRNA vaccine platforms have been developed for a variety of different approaches and targets for flavivirus. mRNA vaccine of DENV, Zika virus and Powassan virus have achieved some progress (Zhang et al., 2020; Wollner et al., 2021; Roth et al., 2019; Pardi et al., 2017; Vanblargan et al., 2018). Studies have confirmed that neutralizing antibody titer does have a protective effect on symptomatic disease after DENV infection (Katzelnick et al., 2016). In most case, specific immune associations appear to be specific to each DENV serotype and vaccine, and the threshold of neutralizing antibodies or cellular immune responses may also be influenced by epidemic-specific infectivity, especially in areas where DENV co-infection is prevalent (Katzelnick et al., 2017). Through humoral and/or cellular immunity, vaccine targets may be ideal for conserved epitopes, but due to the diversity of DENV, ADE may result.

5. Conclusions

In summary, we developed novel mRNA vaccine encoding the E-DIII and NS1 proteins from heterologous viruses. Both DENV mRNA vaccine induced a strong immune response without a severe ADE effect. During the transition from live attenuated vaccine to new vector vaccine, the mRNA vaccine platform has made outstanding contributions to the treatment and prevention of disease. As an alternative strategy to live attenuated DENV vaccine, mRNA vaccine can be engineered to stimulate cellular responses to more conserved non-structural proteins. Future endeavors should focus on the development of an effective vaccine capable of producing an effective protective cross-reaction. The balance between E protein and immunogen structural integrity needs further study. In addition, the persistence of the minimum dose response, validation of the ability of rash to predict vaccination, and the impact of preexisting flavivirus exposure on safety and immunogenicity are highlights that need to be addressed.

Data availability

All the data generated during the current study are included in the manuscript. Further information and requests for resources and reagents should be directed to J.L. and W.L. The DENV sequences were deposited in GenBank with the Accession codes OM403099–OM403102.

Ethics statement

All experiments involving DENV strains were conducted in a biosafety level 2 (BSL2) laboratory, were approved by the Institute of Microbiology, Chinese Academy of Sciences (IMCAS), and complied with all relevant ethical regulations regarding animal research. The animals were housed and bred in specific pathogen-free (SPF) mouse facilities in compliance with ethical guidelines, and all animal experiments were approved by the Experimental Animal Ethics and Welfare Committee of IMCAS.

Author contributions

Lihong He: data curation, formal analysis, investigation, methodology, software, validation, visualization, writing – original draft, writing – review & editing. Wenqiang Sun: investigation, validation. Limin Yang: resources. Wenjun Liu: conceptualization, resources, supervision, funding acquisition. Jing Li: conceptualization, formal analysis, funding acquisition, supervision, visualization, writing – original draft, writing – review & editing.

Conflict of interest

The authors declare no conflict of interest. The funders had no role in the design of the study; in the collection, analyses, or interpretation of data; in the writing of the manuscript, or in the decision to publish the results.

Acknowledgments

Appendix A. Supplementary data

Supplementary data to this article can be found online at https://doi.org/10.1016/j.virs.2022.07.003.

References

Bal, J., Jung, H.Y., Nguyen, L.N., Park, J., Jang, Y.S., Kim, D.H., 2018. Evaluation of cell-surface displayed synthetic consensus dengue EDIII cells as a potent oral vaccine candidate. Microb. Cell Factories 17, 146.

Barban, V., Mantel, N., De Montfort, A., Pagnon, A., Pradezynski, F., Lang, J., Boudet, F., 2018. Improvement of the dengue virus (DENV) nonhuman primate model via a reverse translational approach based on dengue vaccine clinical efficacy data against DENV-2 and -4. J. Virol. 92 e00440–00418.

Beatty, P.R., Puerta-Guardo, H., Killingbeck, S.S., Glasner, D.R., Hopkins, K., Harris, E., 2015. Dengue virus NS1 triggers endothelial permeability and vascular leak that is prevented by NS1 vaccination. Sci. Transl. Med. 7, 304ra141.

Bhamarapravati, N., Sutee, Y., 2000. Live attenuated tetravalent dengue vaccine. Vaccine 18, 44–47.

Biswal, S., Reynales, H., Saez-Llorens, X., Lopez, P., Borja-Tabora, C., Kosalaraksa, P., Sirivichayakul, C., Watanaveeradej, V., Rivera, L., Espinoza, F., Fernando, L., Dietze, R., Luz, K., Venancio Da Cunha, R., Jimeno, J., Lopez-Medina, E., Borkowski, A., Brose, M., Rauscher, M., Lefevre, I., Bizjajeva, S., Bravo, L., Wallace, D., Group, T.S., 2019. Efficacy of a tetravalent dengue vaccine in healthy children and adolescents. N. Engl. J. Med. 381, 2009–2019.

Capeding, R.Z., Luna, I.A., Bomasang, E., Lupisan, S., Lang, J., Forrat, R., Wartel, A., Crevat, D., 2011. Live-attenuated, tetravalent dengue vaccine in children, adolescents and adults in a dengue endemic country: randomized controlled phase I trial in the Philippines. Vaccine 29, 3863–3872.

Chiang, C.Y., Huang, M.H., Hsieh, C.H., Chen, M.Y., Liu, H.H., Tsai, J.P., Li, Y.S., Chang, C.Y., Liu, S.J., Chong, P., Leng, C.H., Chen, H.W., 2012. Dengue-1 envelope protein domain III along with PELC and CpG oligodeoxynucleotides synergistically enhances immune responses. PLoS Neglected Trop. Dis. 6, e1645.

Christofferson Rc, M.M., Johnson, Am, Chisenhall, Dm, Mores, Cn, 2013. Development of a transmission model for dengue virus. Virol. J. 10, 127.

Costa, S.M., Paes, M.V., Barreto, D.F., Pinhao, A.T., Barth, O.M., Queiroz, J.L., Armoa, G.R., Freire, M.S., Alves, A.M., 2006. Protection against dengue type 2 virus

induced in mice immunized with a DNA plasmid encoding the non-structural 1 (NS1) gene fused to the tissue plasminogen activator signal sequence. Vaccine 24, 195–205.

Cui, G., Si, L., Wang, Y., Zhou, J., Yan, H., Jiang, L., 2021. Antibody-dependent enhancement (ADE) of dengue virus: identification of the key amino acid that is vital in DENV vaccine research. J. Gene Med. 23, e3297.

Dai, L., Xu, K., Li, J., Huang, Q., Song, J., Han, Y., Zheng, T., Gao, P., Lu, X., Yang, H., Liu, K., Xia, Q., Wang, Q., Chai, Y., Qi, J., Yan, J., Gao, G.F., 2021. Protective Zika vaccines engineered to eliminate enhancement of dengue infection via immunodominance switch. Nat. Immunol. 22, 958–968.

Dhanoa, A., Hassan, S.S., Ngim, C.F., Lau, C.F., Chan, T.S., Adnan, N.A., Eng, W.W., Gan, H.M., Rajasekaram, G., 2016. Impact of dengue virus (DENV) co-infection on clinical manifestations, disease severity and laboratory parameters. BMC Infect. Dis. 16, 406.

Durbin, A.P., Pierce, K.K., Kirkpatrick, B.D., Grier, P., Sabundayo, B.P., He, H., Sausser, M., Russell, A.F., Martin, J., Hyatt, D., Cook, M., Sachs, J.R., Lee, A.W., Wang, L., Coller, B.A., Whitehead, S.S., 2020. Immunogenicity and safety of a tetravalent recombinant subunit dengue vaccine in adults previously vaccinated with a live attenuated tetravalent dengue vaccine: results of a phase-I randomized clinical trial. Am. J. Trop. Med. Hyg. 103, 855–863.

Elong Ngono, A., Shresta, S., 2019. Cross-reactive T cell immunity to dengue and Zika viruses: new insights into vaccine development. Front. Immunol. 10, 1316.

Golden, J.W., Josleyn, M.D., Hooper, J.W., 2008. Targeting the vaccinia virus L1 protein to the cell surface enhances production of neutralizing antibodies. Vaccine 26, 3507–3515.

Gomes-Ruiz, A.C., Nascimento Rt Fau - De Paula, S.O., De Paula So Fau - Lopes Da Fonseca, B.A., Lopes Da Fonseca, B.A., 2006. SYBR green and TaqMan real-time PCR assays are equivalent for the diagnosis of dengue virus type 3 infections. J. Med. Virol. 78, 760–763.

Grifoni, A., Tian, Y., Sette, A., Weiskopf, D., 2020. Transcriptomic immune profiles of human flavivirus-specific T-cell responses. Immunology 160, 3–9.

Guirakhoo, F., Arroyo, J., Pugachev, K.V., Miller, C., Zhang, Z.X., Weltzin, R., Georgakopoulos, K., Catalan, J., Ocran, S., Soike, K., Ratterree, M., Monath, T.P., 2001. Construction, safety, and immunogenicity in nonhuman primates of a chimeric yellow fever-dengue virus tetravalent vaccine. J. Virol. 75, 7290–7304.

Guy, B., Barban V Fau - Mantel, N., Mantel N Fau - Aguirre, M., Aguirre M Fau - Gulia, S., Gulia S Fau - Pontvianne, J., Pontvianne J Fau - Jourdier, T.-M., Jourdier Tm Fau - Ramirez, L., Ramirez L Fau - Gregoire, V., Gregoire V Fau - Charnay, C., Charnay C Fau - Burdin, N., Burdin N Fau - Dumas, R., Dumas R Fau - Lang, J., Lang, J., 2009. Evaluation of interferences between dengue vaccine serotypes in a monkey model. Am. J. Trop. Med. Hyg. 80, 302–311.

Guzman, M.G., Hermida L Fau - Bernardo, L., Bernardo L Fau - Ramirez, R., Ramirez R Fau - Guillén, G., Guillén, G., 2010. Domain III of the envelope protein as a dengue vaccine target. Expert Rev. Vaccines 9, 137–147.

Jackson, L.A., Rupp, R., Papadimitriou, A., Wallace, D., Raanan, M., Moss, K.J., 2018. A phase 1 study of safety and immunogenicity following intradermal administration of a tetravalent dengue vaccine candidate. Vaccine 36, 3976–3983.

Jearanaiwitayakul, T., Sunintaboon, P., Chawengkittikul, R., Limthongkul, J., Midoeng, P., Warit, S., Ubol, S., 2020. Nanodelivery system enhances the immunogenicity of dengue-2 nonstructural protein 1, DENV-2 NS1. Vaccine 38, 6814–6825.

Katzelnick, L.C., Harris, E., Participants in the Summit on Dengue Immune Correlates Of Protection, 2017. Immune correlates of protection for dengue: state of the art and research agenda. Vaccine 35, 4659–4669.

Katzelnick, L.C., Montoya, M., Gresh, L., Balmaseda, A., Harris, E., 2016. Neutralizing antibody titers against dengue virus correlate with protection from symptomatic infection in a longitudinal cohort. Proc. Natl. Acad. Sci. U. S. A. 113, 728–733.

Khetarpal, N., Khanna, I., 2016. Dengue fever: causes, complications, and vaccine strategies. J. Immunol. Res. 2016, 1–14.

Kim, M.Y., Copland, A., Nayak, K., Chandele, A., Ahmed, M.S., Zhang, Q., Diogo, G.R., Paul, M.J., Hofmann, S., Yang, M.S., Jang, Y.S., Ma, J.K., Reljic, R., 2018. Plant-expressed Fc-fusion protein tetravalent dengue vaccine with inherent adjuvant properties. Plant Biotechnol. J 16, 1283–1294.

Kirkpatrick, B.D., Durbin, A.P., Pierce, K.K., Carmolli, M.P., Tibery, C.M., Grier, P.L., Hynes, N., Diehl, S.A., Elwood, D., Jarvis, A.P., Sabundayo, B.P., Lyon, C.E., Larsson, C.J., Jo, M., Lovchik, J.M., Luke, C.J., Walsh, M.C., Fraser, E.A., Subbarao, K., Whitehead, S.S., 2015. Robust and balanced immune responses to all 4 dengue virus serotypes following administration of a single dose of a live attenuated tetravalent dengue vaccine to healthy, flavivirus-naive adults. J. Infect. Dis. 212, 702–710.

Kirkpatrick, B.D., Whitehead, S.S., Pierce, K.K., Tibery, C.M., Grier, P.L., Hynes, N.A., Larsson, C.J., Sabundayo, B.P., Talaat, K.R., Janiak, A., Carmolli, M.P., Luke, C.J., Diehl, S.A., Durbin, A.P., 2016. The live attenuated dengue vaccine TV003 elicits complete protection against dengue in a human challenge model. Sci. Transl. Med. 8, 330–336.

Liu, Y., Zhang, Y., Wei, Y., Jia, X., Chen, Q., Liu, W., Yang, L., 2020. Development and characterization of serotype-specific monoclonal antibodies against Dengue virus NS1. Sheng Wu Gong Cheng Xue Bao 36, 2206–2215 (In Chinese).

Martinez, D.R., Metz, S.W., Baric, R.S., 2021. Dengue vaccines: the promise and pitfalls of antibody-mediated protection. Cell. Host Microbe. 29, 13–22.

Maruggi, G., Zhang, C., Li, J., Ulmer, J.B., Yu, D., 2019. mRNA as a transformative Technology for vaccine development to control infectious diseases. Mol. Ther. 27, 757–772.

Matangkasombut, P., Manopwisedjaroen, K., Pitabut, N., Thaloengsok, S., Suraamornkul, S., Yingtaweesak, T., Duong, V., Sakuntabhai, A., Paul, R.,

Singhasivanon, P., 2020. Dengue viremia kinetics in asymptomatic and symptomatic infection. Int. J. Infect. Dis. 101, 90–97.

Milligan, G.N., Sarathy, V.V., White, M.M., Greenberg, M.B., Campbell, G.A., Pyles, R.B., Barrett, A.D.T., Bourne, N., 2017. A lethal model of disseminated dengue virus type 1 infection in AG129 mice. J. Gen. Virol. 98, 2507–2519.

Mishra, B., Turuk, J., Sahu, S.J., Khajuria, A., Kumar, S., Dey, A., Praharaj, A.K., 2017. Co-circulation of all four dengue virus serotypes: first report from Odisha. Indian J. Med. Microbiol. 35, 293–295.

Modhiran, N., Watterson, D., Muller, D.A., Panetta, A.K., Sester, D.P., Liu, L., Hume, D.A., Stacey, K.J., Young, P.R., 2015. Dengue virus NS1 protein activates cells via Toll-like receptor 4 and disrupts endothelial cell monolayer integrity. Sci. Transl. Med. 7, 304ra142.

Nivarthi, U.K., Swanstrom, J., Delacruz, M.J., Patel, B., Durbin, A.P., Whitehead, S.S., Kirkpatrick, B.D., Pierce, K.K., Diehl, S.A., Katzelnick, L., Baric, R.S., De Silva, A.M., 2021. A tetravalent live attenuated dengue virus vaccine stimulates balanced immunity to multiple serotypes in humans. Nat. Commun. 12, 1102.

Oberli, M.A., Reichmuth, A.M., Dorkin, J.R., Mitchell, M.J., Fenton, O.S., Jaklenec, A., Anderson, D.G., Langer, R., Blankschtein, D., 2017. Lipid nanoparticle assisted mRNA delivery for potent cancer immunotherapy. Nano Lett. 17, 1326–1335.

Okimoto, T., Friedmann, T., Miyanohara, A., 2001. VSV-G envelope glycoprotein forms complexes with plasmid DNA and MLV retrovirus-like particles in cell-free conditions and enhances DNA transfection. Mol. Ther. 4, 232–238.

Pardi, N., Hogan, M.J., Pelc, R.S., Muramatsu, H., Andersen, H., Demaso, C.R., Dowd, K.A., Sutherland, L.L., Scearce, R.M., Parks, R., Wagner, W., Granados, A., Greenhouse, J., Walker, M., Willis, E., Yu, J.S., Mcgee, C.E., Sempowski, G.D., Mui, B.L., Tam, Y.K., Huang, Y.J., Vanlandingham, D., Holmes, V.M., Balachandran, H., Sahu, S., Lifton, M., Higgs, S., Hensley, S.E., Madden, T.D., Hope, M.J., Kariko, K., Santra, S., Graham, B.S., Lewis, M.G., Pierson, T.C., Haynes, B.F., Weissman, D., 2017. Zika virus protection by a single low-dose nucleoside-modified mRNA vaccination. Nature 543, 248–251.

Paudel, D., Jarman, R., Limkittikul, K., Klungthong, C., Chamnanchanunt, S., Nisalak, A., Gibbons, R., Chokejindachai, W., 2011. Comparison of real-time SYBR green dengue assay with real-time taqman RT-PCR dengue assay and the conventional nested PCR for diagnosis of primary and secondary dengue infection. N. Am. J. Med. Sci. 3, 478–485.

Plummer, E., Shresta, S., 2014. Animal models in dengue. Methods Mol. Biol. 1138, 377–390.

Pokidysheva, E., Zhang, Y., Battisti, A.J., Bator-Kelly, C.M., Chipman, P.R., Xiao, C., Gregorio, G.G., Hendrickson, W.A., Kuhn, R.J., Rossmann, M.G., 2006. Cryo-EM reconstruction of dengue virus in complex with the carbohydrate recognition domain of DC-SIGN. Cell 124, 485–493.

Rai, P., Kille, S., Kotian, A., Kumar, B.K., Deekshit, V.K., Ramakrishna, M.S., Karunasagar, I., Karunasagar, I., 2021. Molecular investigation of the dengue outbreak in Karnataka, South India, reveals co-circulation of all four dengue virus serotypes. Infect. Genet. Evol. 92, 104880.

Ranieri, E., Popescu, I., Gigante, M., 2014. CTL ELISPOT assay. In: RANIERI, E. (Ed.), Cytotoxic T-Cells: Methods and Protocols. Springer New York, New York, NY.

Reddy, P.B., Pattnaik P Fau - Tripathi, N.K., Tripathi Nk Fau - Srivastava, A., Srivastava a Fau - Rao, P.V.L., Rao, P.V., 2012. Expression, purification and evaluation of diagnostic potential and immunogenicity of dengue virus type 3 domain III protein. Protein Pept. Lett. 19, 509–519.

Richner, J.M., Himansu, S., Dowd, K.A., Butler, S.L., Salazar, V., Fox, J.M., Julander, J.G., Tang, W.W., Shresta, S., Pierson, T.C., Ciaramella, G., Diamond, M.S., 2017a. Modified mRNA vaccines protect against Zika virus infection. Cell 168, 1114–1125 e1110.

Richner, J.M., Jagger, B.W., Shan, C., Fontes, C.R., Dowd, K.A., Cao, B., Himansu, S., Caine, E.A., Nunes, B.T.D., Medeiros, D.B.A., Muruato, A.E., Foreman, B.M., Luo, H., Wang, T., Barrett, A.D., Weaver, S.C., Vasconcelos, P.F.C., Rossi, S.L., Ciaramella, G., Mysorekar, I.U., Pierson, T.C., Shi, P.Y., Diamond, M.S., 2017b. Vaccine mediated protection against Zika virus-induced congenital disease. Cell 170, 273–283 e212.

Roth, C., Cantaert, T., Colas, C., Prot, M., Casademont, I., Levillayer, L., Thalmensi, J., Langlade-Demoyen, P., Gerke, C., Bahl, K., Ciaramella, G., Simon-Loriere, E., Sakuntabhai, A., 2019. A modified mRNA vaccine targeting immunodominant NS epitopes protects against dengue virus infection in HLA class I transgenic mice. Front. Immunol. 10, 1424.

Sabchareon, A., Wallace, D., Sirivichayakul, C., Limkittikul, K., Chanthavanich, P., Suvannadabba, S., Jiwariyavej, V., Dulyachai, W., Pengsaa, K., Wartel, T.A., Moureau, A., Saville, M., Bouckenooghe, A., Viviani, S., Tornieporth, N.G., Lang, J., 2012. Protective efficacy of the recombinant, live-attenuated, CYD tetravalent dengue vaccine in Thai schoolchildren: a randomised, controlled phase 2b trial. Lancet 380, 1559–1567.

Sáez-Llorens, X., Tricou, V., Yu, D., Rivera, L., Jimeno, J., Villarreal, A.C., Dato, E., Mazara, S., Vargas, M., Brose, M., Rauscher, M., Tuboi, S., Borkowski, A., Wallace, D., 2018. Immunogenicity and safety of one versus two doses of tetravalent dengue vaccine in healthy children aged 2-17 years in Asia and Latin America: 18-month interim data from a phase 2, randomised, placebo-controlled study. Lancet Infect. Dis. 18, 162–170.

Sarathy, V.V., Milligan, G.N., Bourne, N., Barrett, A.D., 2015. Mouse models of dengue virus infection for vaccine testing. Vaccine 33, 7051–7060.

Shi, B., Xue, M., Wang, Y., Wang, Y., Li, D., Zhao, X., Li, X., 2018. An improved method for increasing the efficiency of gene transfection and transduction. Int. J. Physiol. Pathophysiol. Pharmacol. 10, 95–104.

Sirivichayakul, C., Barranco-Santana, E.A., Esquilin-Rivera, I., Oh, H.M., Raanan, M., Sariol, C.A., Shek, L.P., Simasathien, S., Smith, M.K., Velez, I.D., Wallace, D., Gordon, G.S., Stinchcomb, D.T., 2016. Safety and immunogenicity of a tetravalent

dengue vaccine candidate in healthy children and adults in dengue-endemic regions: a randomized, placebo-controlled phase 2 study. J. Infect. Dis. 213, 1562–1572.

Thomas, A., Thiono, D.J., Kudlacek, S.T., Forsberg, J., Premkumar, L., Tian, S., Kuhlman, B., De Silva, A.M., Metz, S.W., 2020. Dimerization of dengue virus E subunits impacts antibody function and domain focus. J. Virol. 94, e00745–00720.

Vanblargan, L.A., Himansu, S., Foreman, B.M., Ebel, G.D., Pierson, T.C., Diamond, M.S., 2018. An mRNA vaccine protects mice against multiple tick-transmitted flavivirus infections. Cell Rep. 25, 3382–3392. e3383.

Wollner, C.J., Richner, J.M., 2021. mRNA vaccines against flaviviruses. Vaccines 9, 1464.

Wollner, C.J., Richner, M., Hassert, M.A., Pinto, A.K., Brien, J.D., Richner, J.M., 2021. A dengue virus serotype 1 mRNA-LNP vaccine elicits protective immune responses. J. Virol. 95, e02482-20.

Yanez Arteta, M., Kjellman, T., Bartesaghi, S., Wallin, S., Wu, X., Kvist, A.J., Dabkowska, A., Szekely, N., Radulescu, A., Bergenholtz, J., Lindfors, L., 2018. Successful reprogramming of cellular protein production through mRNA delivered by functionalized lipid nanoparticles. Proc. Natl. Acad. Sci. U. S. A. 115, E3351–E3360.

Zhang, M., Sun, J., Li, M., Jin, X., 2020. Modified mRNA-LNP vaccines confer protection against experimental DENV-2 infection in mice. Mol. Ther. Methods Clin. Dev. 18, 702–712.

Zuest, R., Valdes, I., Skibinski, D., Lin, Y., Toh, Y.X., Chan, K., Hermida, L., Connolly, J., Guillen, G., Fink, K., 2015. Tetravalent dengue DIIIC protein together with alum and ODN elicits a Th1 response and neutralizing antibodies in mice. Vaccine 33, 1474–1482.